High-energy square pulses and burst-mode pulses in an all-normal dispersion double-clad mode-locked fiber laser

2016 Appl. Phys. Express 9 052701

(http://iopscience.iop.org/1882-0786/9/5/052701)

Applied Physics Express **9**, 052701 (2016)
http://doi.org/10.7567/APEX.9.052701

High-energy square pulses and burst-mode pulses in an all-normal dispersion double-clad mode-locked fiber laser

Zhi Qiao[1,2], Xiaochao Wang[1*], Chao Wang[1,2], Yuanyuan Jing[1,2], Wei Fan[1*], and Zunqi Lin[1]

[1]*National Laboratory on High Power Lasers and Physics, Shanghai Institute of Optics and Fine Mechanics, Chinese Academy of Science, Shanghai 201800, China*
[2]*University of the Chinese Academy of Sciences, Beijing 100049, China*

*E-mail: smilexc@siom.ac.cn; fanweil@siom.ac.cn

Received March 8, 2016; accepted March 30, 2016; published online April 14, 2016

A double-clad Yb-doped mode-locked fiber laser that can operate in burst-mode and square-pulse states is experimentally investigated. In the burst-mode state, a burst train with 55 pulses of 500 ps duration is obtained. In the square-pulse state, which is similar to noiselike pulses, the maximum pulse energy is 820 nJ and the duration can be tuned from 15.8 to 546 ns. The square pulses have a narrow and multipeak spectrum, which is quite different from that of normal noiselike pulses. The fiber laser promises an alternative formation mechanism for burst-mode and square-pulse mode-locked fiber lasers.

Over the past two decades, passive mode-locked fiber lasers have attracted considerable interest because of their various applications in industrial and scientific fields.[1)] Conventional solitons in mode-locked fiber lasers with anomalous dispersion depend on the balance between the nonlinear effect and the group velocity dispersion (GVD).[2)] However, the pulse energy is restricted by the wave breaking effect in a mode-locked fiber laser. A higher pulse energy is desired to obtain better performance in material processing, biology, telecommunication, and nonlinear physics. Dissipative solitons (DSs), being different from conventional solitons, can provide a higher pulse energy and have attracted much attention.[3–8)] Nevertheless, high-order nonlinear effects, the wave breaking effect, and multipulsing instability (MPI) still restrict the highest pulse energy of DSs to tens of nanojoules.[9–12)]

New soliton formation mechanisms, i.e., noiselike rectangular pulses, have been proposed recently to obtain mode-locked pulses with higher energy.[13)] The duration and single-pulse energy of noiselike pulses can both increase to very large values with constant amplitude.[14)] Besides that, the noiselike pulses are a compact and convenient way of producing high-energy square nanosecond pulses, which are usually generated by a pulse-shaping system combined with several amplifiers.[15)] Compared with normal mode-locked pulses, the most attractive property of noiselike pulses is the incoherence. In laser ignition facilities such as the National Ignition Facility (NIF), Laser Mégajoule (LMJ), and ShengGuang (SG) series, the laser pulse is phase-modulated by sinusoidal signals to suppress stimulated Brillouin scattering and obtain smooth focal spots on the target.[16)] However, the phase-modulated pulse is still coherent; thus, it is extremely difficult to obtain smooth focal spots. The incoherent noiselike pulses are a promising method of fulfilling the increasing need for physical experiments. Noiselike pulses have been widely investigated in Er-doped fiber lasers, and various studies have been conducted on their formation mechanism.[13,17)] However, few studies have been carried out on Yb-doped fiber (YDF) lasers, and most noiselike pulses have been shown to have broad spectra owing to high peak powers or the Raman effect.[18–21)] It is important to determine whether it is possible to form pulses, similar to the noiselike rectangular pulses, with long durations and low peak powers in YDF lasers without the Raman effect.

In this paper, we demonstrate a nonlinear polarization rotation (NPR) technique-based mode-locked fiber laser where a double-clad Yb-doped gain fiber is utilized to support a higher pump power. Two mode-locked outputs, burst-mode DSs and square pulses, coexist in the mode-locked fiber laser. With a proper polarization state in the cavity, the burst-mode DSs were obtained at a repetition frequency of 196 kHz with a maximum pulse number of 55. The pulse number and center wavelength could be easily tuned by changing the pump power while keeping the amplitude of the pulse train constant. The burst-mode DSs are actually induced by the multipulsing effect in the DS fiber laser and have potential applications in micromachining.[22–24)] Aside from the burst-mode DSs, square pulses, which are similar to noiselike pulses, were also obtained. By increasing the pump power, the square pulse width could be tuned from 15.8 to 546 ns with a maximum pulse energy of 820 nJ at a repetition frequency of 196 kHz. The spectra of the square pulses were quite different from those of the normal noiselike pulses. Several narrow peaks occurred in the former compared with a broad spectrum in the noiselike pulse state. The pulse energy and duration of square pulses are the highest and largest reported direct outputs from a fiber laser to the best of our knowledge, and we show that square pulses, which are similar to noiselike pulses, can exist without the Raman effect at low peak powers.[17)] The mode-locked fiber laser shows potential applications in burst-mode sources and incoherent nanosecond seeding laser systems.

The schematic of the mode-locked fiber laser is shown in Fig. 1. The cavity consisted of a segment of 4 m double-clad Yb-doped fibers (YDFs), a polarization-independent isolator (ISO), a piece of 1 km single-mode fiber (SMF; 1060XP), two polarization controllers (PCs), an in-line polarizer (ILP), a 95% output coupler (OC), and a pump combiner. The double-clad Yb-doped fiber (Nufern, 5/130 μm) was cladding-pumped by a pigtailed fiber laser diode with a maximum power of 6.5 W at 976 nm. All elements were made of a normal single-mode fiber (HI1060), and the total dispersion of the cavity was estimated at ∼23 ps^2, which is quite large for a mode-locked fiber laser. Another two fiber couplers with 10 and 50% output ratios were utilized to monitor the waveform, spectrum, and average power simultaneously. The spectrum of the mode-locked laser was measured using an optical spectrum analyzer (Yokogawa AQ6370B), and

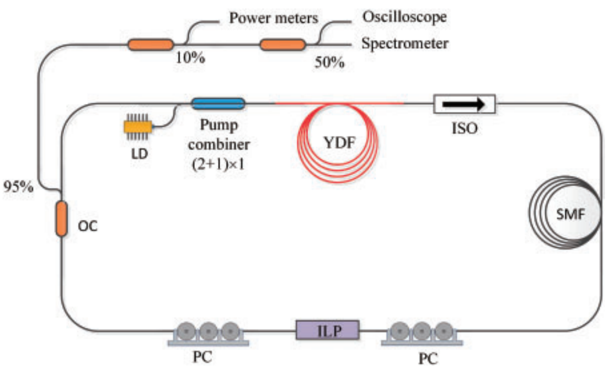

Fig. 1. Schematic of the mode-locked fiber laser. SMF: single-mode fiber; LD: laser diode; PC: polarization controller; ISO: polarization-independent isolator; ILP: in-line polarizer; OC: output coupler; YDF: Yb-doped fiber.

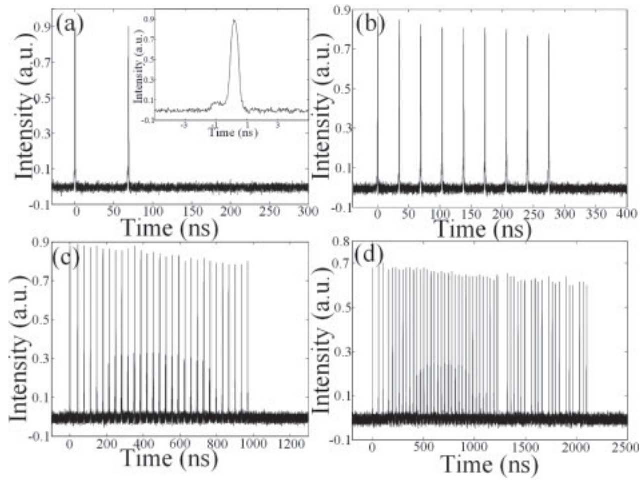

Fig. 2. Evolution of pulse trains with pump power in the burst-mode dissipative soliton region. (a) Two pulses in one burst train with a pump power of 2.3 W; (b) 9 pulses in one burst train with a pump power of 2.8 W; (c) 29 pulses in one burst train with a pump power of 4 W; (d) 55 pulses in one burst train with a pump power of 4.7 W.

the waveform was acquired with a 12 GHz oscilloscope (Tektronics DPO71254C) together with a 5 GHz photoelectric detector (Thorlabs DET08FC).

The stable burst-mode state starts with twin pulses at a pump power of 2.3 W, as shown in Fig. 2(a). The single pulse in the sequence has a duration of about 0.5 ns, and the distance between the twin pulses is 68 ns. The repetition rate of the pulse train is 196 kHz corresponding to a pulse interval of 5.1 µs. When the pump power is increased to 2.8 and 4 W, the pulse number of the train in Figs. 2(b) and 2(c) gradually increases to 9 and 29 with almost the same amplitude and pulse shape, respectively, and the pulse temporal distance decreases compared with the state at 2.3 W. The pulse number can be further increased by increasing the pump power, and the maximum pulse number is 55 at a pump power of 4.7 W, as shown in Fig. 2(d). A slight hysteresis phenomenon is observed, which is coincident with previous results.[25] It can be seen that the amplitude of pulses in the sequence shown in Fig. 2(d) decreases gradually, which is the result of the gain saturation effect, that is, the last pulses in the sequence experience less gain and lower saturated energy. A few pulses in the sequence vanish in Fig. 2(d) and the temporal distance varies from pulse to pulse in the high-pump-power mode-locked state. The pulse train

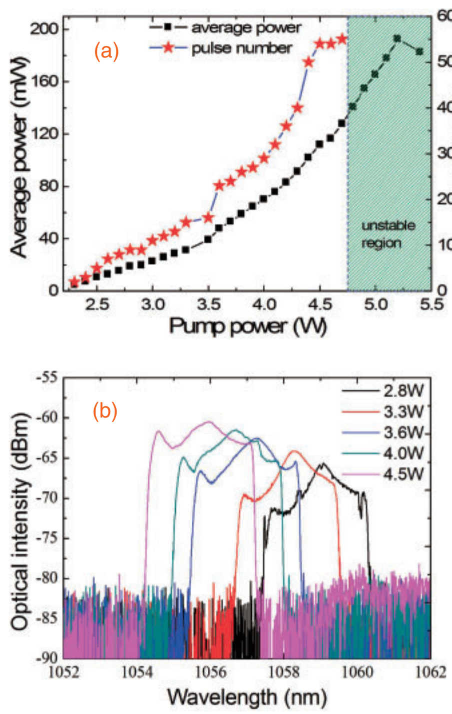

Fig. 3. (a) Average power and pulse numbers of burst-mode pulses with different pump powers. (b) Spectrum of burst-mode pulses at different pump powers.

can also be adjusted by PCs in the cavity to make some pulses in the sequence appear or disappear, which promises a potential application in flexible burst-mode fiber lasers.

The average output power and pulse number of the train at different pump powers are shown in Fig. 3(a). The total average output power and pulse number in one sequence increase along with the pump power. With a pump power of 4.7 W, the maximum average output power is 128 mW and the pulse number is 55. The pulse energy of a single pulse in one pulse train is about 12 nJ. The pulse numbers as well as the output powers are not linearly but exponentially related to the pump power, which differs from early theoretical results.[25] As shown in Fig. 3(a), the relationship is approximately linear only when the pump power is lower than 3.5 W, where the pulse number is less than 10. When the pump power is further increased to 4.8 W, the output pulse train becomes unstable.

The spectrum of the pulse train is shown in Fig. 3(b) with different pump powers. The spectrum shows a steep edge that is a typical feature in dissipative soliton spectra. The spectral width (FWHM) is 2.7 nm and does not change with pump power. When the pump power is tuned from 2.8 to 4.5 W, the center wavelength of output pulses decreases from 1059 to 1056 nm.

The output pulse train is actually due to the multipulsing effect of dissipative solitons. The pulse number can be simply tuned from 2 to 55 by increasing or decreasing the pump power in this double-clad mode-locked fiber laser. The output train is the same as that with the pulse of a laser system working in the burst mode, and one advantage of this burst-mode mode-locked fiber laser is that the output pulse is linearly chirped and has a relatively long duration, which can be directly applied in high-power chirped pulse amplification (CPA) systems working in the burst mode without the

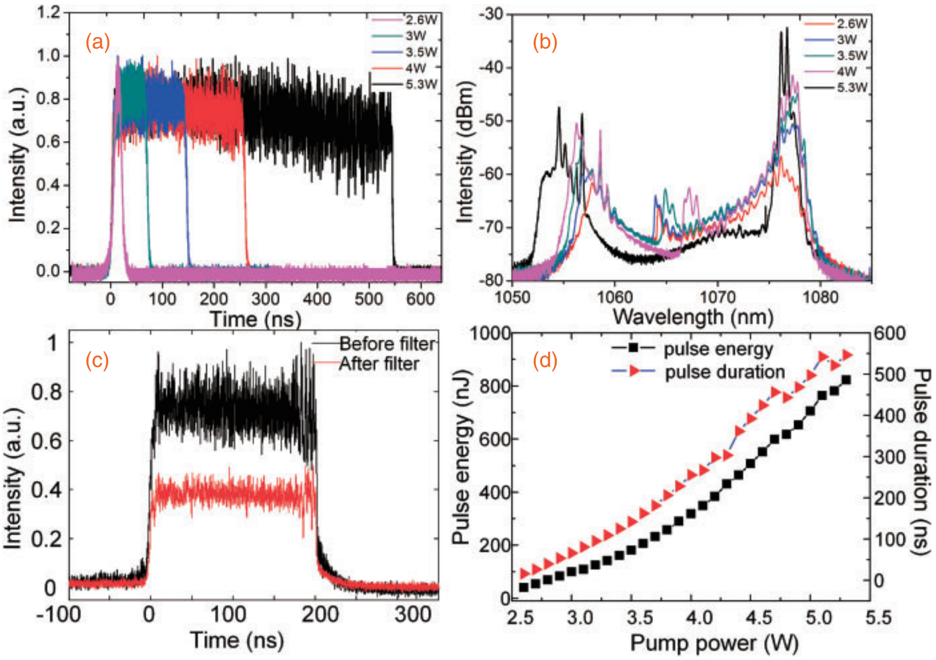

Fig. 4. (a) Evolution of the single square pulse under different pump powers. (b) Spectrum of square pulses with different pump powers. (c) Temporal profile of square pulses before (black line) and after (red line) the spatial spectral filter. (d) Pulse energy and duration of square pulses with different pump powers.

prestretching stage. The wavelength-tunable mode-locked fiber laser also provides more flexibility in high-power burst-mode systems. The results show that this mode-locked fiber laser can be used as a burst-mode oscillator to obtain a higher single pulse energy in amplifiers. The amplification of this burst-mode mode-locked fiber laser will be a subject of future work.

Stable square pulses can be obtained at the fundamental repetition frequency of 196 kHz. It is interesting that the square-pulse state can be achieved by slightly adjusting the PCs in the cavity when burst-mode dissipative solitons are formed, indicating that the two states have similar cavity conditions. The evolution of typical square pulses under different pump powers is shown in Fig. 4(a). It can be seen that the amplitude of square pulses is almost constant when the pulse duration increases with pump power, which is the same as that of noiselike pulses. The square pulses in Fig. 4(a) show picosecond fine structures, which vary randomly with time. The square pulses were measured again using a 30 GHz oscilloscope and a 45 GHz photoelectric detector (Newport 1014), and the temporal profile is just like that shown in Fig. 4(a). Therefore, it is reasonable to consider that the square pulses consist of picosecond pulses similarly to the noiselike pulses. Because of the large positive dispersion in the cavity, the picosecond pulses in the square pulses can separate temporally and be acquired by the oscilloscope. The spectrum evolution with changing pump power is shown in Fig. 4(b). There is no steep edge in the spectrum, which is different from the spectrum of the DSs in Fig. 3(b). Generally, noiselike pulses have a broad spectrum that can be as broad as 70 nm. However, the spectrum in Fig. 4(b) is narrow and has several peaks, which is different from the spectra of the normal noiselike pulses. To confirm whether the square pulses are actually noiselike pulses, the square pulses are examined using an autocorrelator (APE Pulsecheck-150). Nevertheless, no coherence spike, which is a typical feature of noiselike pulses, is observed. To further investigate the characteristics of the waveform and spectrum, the square pulses are transmitted into a spatial spectral filter based on two gratings (1800 line/mm) that can separate the peaks of the spectrum in space. The two gratings are aligned parallel to form a stretcher such that the square pulse can be chirped spatially. Owing to the diffraction of gratings, different parts of the spectrum can be separated in space and measured using a photoelectric detector together with a pinhole. As shown in Fig. 4(b), two main peaks exist in the spectrum and two obvious spots can be observed in the experiment after two parallel gratings. The square pulses are measured at different positions in space with a 5 GHz spatial photoelectric detector (Thorlabs DET08C). The measured temporal profile shows no difference, as shown in Fig. 4(c), where the typical waveform after the spatial spectral filter (red line) is compared with that before the filter (black line). Furthermore, the square pulses are also examined using a simple Mach–Zehnder (MZ) interferometer and no interference phenomenon is observed. The fact that the temporal profile of square pulses is independent of the spectrum proves that the square pulses are incoherent. The square pulses are also transmitted in a 2-km-long single-mode fiber and no wave-breaking effect is observed.

The single pulse energy and pulse duration under different pump powers are shown in Fig. 4(d). The single pulse energy increases almost linearly with pump power. At a pump power of 5.3 W, the average output power is 161 mW corresponding to a single pulse energy of 820 nJ, where the square pulse duration is 546 ns. By increasing the pump power, the duration of the square pulse can be tuned from 15.8 to 546 ns. In the experiment, when the pump power exceeds 5.3 W, the square pulses evolve into the second-harmonic mode-locking state that is coincident with the behavior of normal noiselike pulses. The stability of the output power is about 1% (rms) over 3 h. The pulse energy and duration are the highest reported as direct outputs from a square-pulse mode-locked all-fiber laser to the best of our knowledge. The pulse duration can also be tuned by PCs in the cavity at a certain pump power, which is flexible in some applications.

In conclusion, a double-clad Yb-doped mode-locked fiber laser generating both burst-mode dissipative solitons and square pulses is experimentally investigated. Stable pulse trains in the DS region are obtained and as much as 55 pulses with a single pulse energy of 12 nJ exist in one burst sequence. The pulse numbers in one sequence can be changed by simply adjusting the pump power. The pulses with temporally equal distances in one train are suitable for working in the burst mode for high-power amplifiers owing to their long duration, stable passive structure, and compressible linear chirp characteristic. By changing slightly the polarization state in the cavity, square pulses are obtained. The narrow and multipeak spectrum of square pulses is quite different from that of normal noiselike pulses. However, the square pulses are examined using a simple spatial spectral filter, and the results show that the temporal profile is independent of the spectrum. Other similar characteristics such as the constant amplitude, square profile, and picosecond fine structures indicate that the square pulses are incoherent and the same as the noiselike pulses. The maximum single pulse energy of the square pulse is 820 nJ, which is the highest reported energy of a single square pulse in a square-pulse mode-locked fiber laser. The square-pulse duration can be tuned from 15.8 to 546 ns by increasing the pump power. It is shown that the double-clad mode-locked fiber laser can support both burst-mode operation in the DS region and incoherent square pulses with higher energy and larger duration, which have potential applications in burst-mode sources and incoherent nanosecond front systems in large laser facilities. The low peak power and square pulses that have the same features as noiselike pulses will be helpful for further understanding the formation of noiselike pulses without the Raman effect. Furthermore, the results provide an alternative to obtaining burst-mode and square pulses.

Acknowledgment This work is supported by the National Natural Science Foundation of China (Grant No. 61205103).

1) B. Oktem, C. Ülgüdür, and F. Ilday, Nat. Photonics **4**, 307 (2010).
2) F. W. Wise, A. Chong, and W. Renninger, Laser Photonics Rev. **2**, 58 (2008).
3) B. Ortaç, M. Plötner, T. Schreiber, J. Limpert, and A. Tünnermann, Opt. Express **15**, 15595 (2007).
4) W. Renninger, A. Chong, and F. Wise, Opt. Lett. **33**, 3025 (2008).
5) M. Fermann, V. Kruglov, B. Thomsen, J. Dudley, and J. Harvey, Phys. Rev. Lett. **84**, 6010 (2000).
6) V. Kruglov, A. Peacock, and J. Harvey, Phys. Rev. Lett. **90**, 113902 (2003).
7) P. Li, L. Shi, Q. Sun, J. Wang, and Q. Mao, Chin. Opt. Lett. **13**, 031403 (2015).
8) X. Yang, Y. Chen, C. Zhao, and H. Zhang, Chin. Opt. Lett. **12**, 031405 (2014).
9) G. Z. Zhao, X. S. Xiao, J. W. Mei, and C. X. Yang, Chin. Phys. Lett. **29**, 034207 (2012).
10) J.-H. Lin and K.-H. Lin, J. Phys. B **43**, 065402 (2010).
11) X. Liu, Opt. Express **17**, 22401 (2009).
12) M. Abdelalim, Y. Logvin, D. Khalil, and H. Anis, Opt. Express **17**, 13128 (2009).
13) X. W. Zheng, Z. C. Luo, H. Liu, N. Zhao, Q. Y. Ning, M. Liu, X.-H. Feng, X.-B. Xing, A.-P. Luo, and W.-C. Xu, Appl. Phys. Express **7**, 042701 (2014).
14) Y. Jeong, L. A. Vazquez-Zuniga, S. Lee, and Y. Kwon, Opt. Fiber Technol. **20**, 575 (2014).
15) Z. Qiao, X. Wang, W. Fan, and Z. Lin, Opt. Lett. **40**, 4214 (2015).
16) A. Jolly, J. Gleyze, J. Luce, H. Coic, and G. Deschaseaux, Opt. Eng. **42**, 1427 (2003).
17) J. Liu, Y. Chen, P. Tang, C. Xu, C. Zhao, H. Zhang, and S. Wen, Opt. Express **23**, 6418 (2015).
18) H. Chen, S. Chen, Z. Jiang, and J. Hou, Opt. Lett. **40**, 5490 (2015).
19) A. K. Zaytsev, C. H. Lin, Y. J. You, F. H. Tsai, C. L. Wang, and C. L. Pan, Laser Phys. Lett. **10**, 045104 (2013).
20) M. Suzuki, R. A. Ganeev, S. Yoneya, and H. Kuroda, Opt. Lett. **40**, 804 (2015).
21) D. Li, D. Shen, L. Li, H. Chen, D. Tang, and L. Zhao, Opt. Express **23**, 25889 (2015).
22) S. Rezaei, J. Li, and P. Herman, Opt. Lett. **40**, 2064 (2015).
23) R. Woodward, E. Kelleher, T. Runcorn, S. Loranger, D. Popa, V. Wittwer, A. Ferrari, S. Popov, R. Kashyap, and J. Taylor, Opt. Lett. **40**, 387 (2015).
24) Y. Ma, Y. He, X. Yu, X. Li, J. Li, R. Yan, J. Peng, X. Zhang, R. Sun, Y. Pan, and D. Chen, Opt. Express **23**, 24955 (2015).
25) X. Liu, Phys. Rev. A **81**, 023811 (2010).